

## Review article

# Stress Computed Tomography Myocardial Perfusion Imaging: A New Topic in Cardiology



Sara Seitun,<sup>a,\*</sup> Margherita Castiglione Morelli,<sup>a</sup> Irilda Budaj,<sup>a</sup> Sara Boccalini,<sup>a</sup> Athena Galletto Pregliasco,<sup>a</sup> Alberto Valbusa,<sup>b</sup> Filippo Cademartiri,<sup>c</sup> and Carlo Ferro<sup>a</sup>

<sup>a</sup> Department of Radiology, Interventional Radiology, IRCCS San Martino University Hospital-IST, National Institute for Cancer Research, Genoa, Italy

<sup>b</sup> Department of Cardiology, IRCCS San Martino University Hospital-IST, National Institute for Cancer Research, Genoa, Italy

<sup>c</sup> Department of Radiology, Cardiology, Erasmus Medical Center University, Rotterdam, The Netherlands

Article history:

Available online 14 January 2016

Keywords:

Computed tomography myocardial perfusion

Stress computed tomography

Dual-energy computed tomography

Myocardial perfusion imaging

## ABSTRACT

Since its introduction about 15 years ago, coronary computed tomography angiography has become today the most accurate clinical instrument for noninvasive assessment of coronary atherosclerosis. Important technical developments have led to a continuous stream of new clinical applications together with a significant reduction in radiation dose exposure. Latest generation computed tomography scanners ( $\geq 64$  slices) allow the possibility of performing static or dynamic perfusion imaging during stress by using coronary vasodilator agents (adenosine, dipyridamole, or regadenoson), combining both functional and anatomical information in the same examination. In this article, the emerging role and state-of-the-art of myocardial computed tomography perfusion imaging are reviewed and are illustrated by clinical cases from our experience with a second-generation dual-source 128-slice scanner (Somatom Definition Flash, Siemens; Erlangen, Germany). Technical aspects, data analysis, diagnostic accuracy, radiation dose and future prospects are reviewed.

© 2015 Sociedad Española de Cardiología. Published by Elsevier España, S.L.U. All rights reserved.

## Técnica de imagen de perfusión miocárdica con tomografía computarizada de estrés: un nuevo tema en cardiología

## RESUMEN

Tras su introducción hace unos 15 años, la angiografía por tomografía computarizada se ha convertido actualmente en el instrumento clínico más exacto para la evaluación no invasiva de la aterosclerosis coronaria. Los importantes avances técnicos han conducido a un torrente continuo de nuevas aplicaciones clínicas junto con una reducción significativa de la dosis de exposición a la radiación. Los escáneres de tomografía computarizada de última generación ( $\geq 64$  cortes) brindan la posibilidad de obtener imágenes de perfusión estáticas o dinámicas durante la aplicación de estrés mediante vasodilatadores coronarios (adenosina, dipiridamol o regadenosón), combinando la información funcional y anatómica en la misma exploración. En este artículo se examina el papel emergente y el estado actual de las imágenes de perfusión miocárdica con tomografía computarizada, y se ilustra con casos clínicos de la propia experiencia con un escáner de segunda generación de 128 cortes y doble fuente (Somatom Definition Flash, Siemens; Erlangen, Alemania). Se examinan los aspectos técnicos, el análisis de los datos, la exactitud diagnóstica, la dosis de radiación y las perspectivas futuras.

© 2015 Sociedad Española de Cardiología. Publicado por Elsevier España, S.L.U. Todos los derechos reservados.

Palabras clave:

Perfusión miocárdica con tomografía computarizada

Tomografía computarizada de estrés

Tomografía computarizada de energía dual

Imágenes de perfusión miocárdica

## INTRODUCTION

A number of advances during the last 15 years have seen coronary computed tomography angiography (CTA) become one of the mainstay diagnostic tools for noninvasive assessment of coronary atherosclerosis in patients with a low-to-intermediate probability of coronary artery disease (CAD).<sup>1–4</sup> Coronary CTA

demonstrates high sensitivity and negative predictive value in determining significant stenosis ( $\geq 50\%$  lumen reduction), approaching 100%.<sup>1–4</sup> However, based solely on the morphological characteristics of the coronary lesions, the hemodynamic significance of the stenosis cannot be determined, especially that of intermediate-grade stenosis (40%–70% lumen reduction), as demonstrated by studies of invasive fractional flow reserve (FFR) measurements.<sup>5</sup> The landmark FAME trial has demonstrated that an FFR-guided percutaneous coronary intervention approach is superior to treatment with a percutaneous coronary intervention based solely on visual angiographic assessment of coronary lesions, with an improved clinical outcome and a positive

\* Corresponding author: Department of Radiology and Interventional Radiology, IRCCS San Martino University Hospital-IST, National Institute for Cancer Research, Largo R. Benzi 10, 16132, Genoa, Italy.

E-mail address: saraseitun@yahoo.com (S. Seitun).

### Abbreviations

CAD: coronary artery disease  
 CTA: computed tomography angiography  
 CTP: computed tomography perfusion  
 DE: dual-energy  
 DSCT: dual-source computed tomography  
 MBF: myocardial blood flow  
 MRI: magnetic resonance imaging  
 SPECT: single-photon emission computed tomography

economic impact on health care cost.<sup>5</sup> To date, the 2 largest randomized controlled trials, the COURAGE<sup>6</sup> and BARI 2D<sup>7</sup> trials, have failed to show that percutaneous coronary intervention based solely on a standard visual approach is superior to optimal medical therapy in reducing mortality or recurrent myocardial infarction. Therefore, these studies suggest that functional assessment of coronary lesions may help to identify patients who may benefit from revascularization in stable CAD. Moreover, studies correlating the anatomic information of coronary CTA with single-photon emission computed tomography (SPECT) have demonstrated a moderate positive predictive value (about 50%) of CTA in determining inducible myocardial ischemia.<sup>8,9</sup> For these reasons, in clinical practice, morphological information obtained with coronary CTA often requires integration with functional imaging tests such as SPECT, positron emission tomography, or magnetic resonance imaging (MRI) during pharmacological stress to highlight perfusion defects, with an impact on patient management and prognosis. However, the latest-generation computed tomography (CT) scanners ( $\geq 64$  slices) allow static and dynamic CT perfusion (CTP) to be obtained during stress by using coronary vasodilator agents (adenosine, dipyridamole, or regadenoson), combining both functional and anatomical information in the same examination, which are essential in state-of-the-art patient management.<sup>2,5</sup> In this article, the emerging role and state-of-the-art of myocardial CTP during pharmacological stress are reviewed and illustrated by clinical cases from our preliminary experience with a second-generation 128-slice dual-source CT (DSCT) scanner (Somatom Definition Flash, Siemens; Germany). Technical aspects, data analysis, diagnostic accuracy, radiation dose and the possible future role of this innovation are reviewed.

### PHYSIOPATHOLOGY OF ISCHEMIA

Myocardial perfusion is a highly regulated process influenced by numerous factors, such as epicardial vessels, resistance vessels, and endothelium.<sup>10</sup> At rest, the myocardium oxygen extraction rate is very high (75%–80%) and, whenever demands increase, the myocardium can supply incrementing coronary blood flow and oxygen delivery.<sup>10</sup> Ischemia can occur secondary to reduced coronary blood flow/perfusion pressure not compensated by the autoregulation process, which is the ability to maintain a relatively stable coronary perfusion over a wide range of perfusion pressures due to dilation of resistance vessels. Coronary blood flow at rest is not compromised by epicardial stenosis of up to 85%–90% but, in the presence of maximal hyperemia, it decreases with stenosis of  $> 45\%$ .<sup>10</sup> Moreover, the physiological effect of stenosis also depends on the degree of compensation of the distal microcirculatory bed.<sup>10,11</sup> The ischemic process initially involves the subendocardial layer with an endo-subpericardial front causing a cascade of physiopathological events among which perfusion

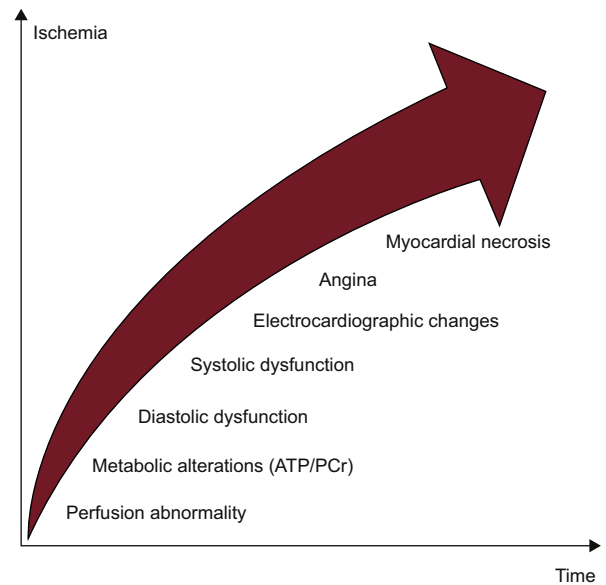


**Figure 1.** The ischemic cascade. ATP/PCr, adenosine triphosphate/phosphocreatine.

reduction is an early change (Figure 1).<sup>10</sup> For these reasons, stress tests evaluating this parameter are more sensitive in identifying hemodynamically significant stenosis than analysis of the stress-induced wall motion abnormalities or electrocardiogram (ECG) changes alone (Figure 1).<sup>10</sup>

### ACQUISITION MODALITY

Myocardial stress CTP images can be acquired in either a static or dynamic mode. Static CTP imaging acquires a single temporal phase during the arterial first-pass of the contrast agent.<sup>12</sup> Among static techniques, the recently introduced dual-energy (DE) acquisition is one of the most promising techniques and consists of the use of different X-ray spectra generated by different tube voltages.<sup>13,14</sup> Dynamic time-resolved CTP acquisition allows the acquisition of multiple consecutive contrast-enhanced phases as the contrast bolus transits the myocardium, in a manner similar to stress-MRI.<sup>12</sup> By obtaining time attenuation curve (TAC) computation, dynamic acquisition enables perfusion parameters to be calculated from mathematical modeling.<sup>9</sup>

#### Monoenergetic Static Acquisition

A single stationary contrast-enhanced first-pass arterial acquisition during pharmacological stress is performed. Optimization of the timing of image acquisition is therefore crucial to acquire the dataset during the peak of myocardial enhancement.<sup>15,16</sup> Several acquisition techniques are available with a progressive reduction in dose profile and contrast media administration: retrospective ECG-gating (with prospective tube current modulation),<sup>17,18</sup> prospective ECG-gating,<sup>19,20</sup> and prospectively ECG-triggered high-pitch spiral acquisition implemented with the second-generation 128-slice DSCT scanner.<sup>21,22</sup>

#### Static Acquisition With the Dual-energy Technique

The DE technique allows quantitative analysis through evaluation of iodine distribution during the first-pass phase of the contrast agents based on their X-ray absorption characteristics

at different X-ray tube voltage settings (kV), which affect the X-ray energy levels.<sup>23</sup> Dual-energy acquisition can be performed with a DSCT scanner with 2 tubes simultaneously emitting higher (140–150 kV) and lower (80–90–100 kV) energy levels.<sup>23,24</sup> A second approach consists of a single-source CT scanner with fast tube voltage switching (from 80 kV to 140 kV) either in a single gantry rotation (GSI Cardiac, GE Healthcare) or in consecutive rotations (Acquilion One, Toshiba).<sup>9</sup> Another possibility still under investigation is the double-layer approach with 2 overlaid detectors made of different materials (Philips Medical Systems prototype).<sup>9</sup>

The introduction of the second-<sup>21</sup> or third-generation<sup>25</sup> DSCT scanners with high temporal resolution (75 ms or 66 ms, respectively) can overcome cardiac motion artifacts of the DE CTP, especially in patients with a high heart rate and high heart rate variability.

### Dynamic Computed Tomography Perfusion Acquisition

Dynamic CTP acquisition allows the quantification of myocardial blood flow and volume and potentially of other hemodynamic parameters, through the mathematical elaboration of TAC.<sup>9</sup> Dynamic CTP imaging requires a sufficiently high temporal resolution to image heart rates at stress and a detector array sufficiently wide to image the entire myocardium in rapid succession. Whole-heart coverage can be achieved using a single-tube scanner with a 256-slice wide-detector CT system while the table is stationary with a coverage of 78 mm,<sup>26</sup> or by using a DSCT scanner with the shuttle mode.<sup>27,28</sup> In the shuttle mode, the table moves back and forth in 2 alternate scanning positions covering a total of 73 mm.<sup>27,28</sup> The newly introduced third-generation DSCT scanner with 192 detectors allows for a wider Z-coverage of 105 mm, with the possibility of also studying larger or dilated hearts.<sup>25</sup> For both modalities (stationary table or shuttle mode), data are acquired for approximately 30 s during the longitudinal systolic shortening of the left ventricle, when the left ventricular myocardium is thicker, providing a more robust set for perfusion analysis. The amount of contrast medium administered is usually 50 mL followed by 50 mL of saline at 5–6 mL/s.<sup>16,27</sup>

### EXAMINATION PROTOCOL

Combined coronary CTA and CTP protocols can be performed with a rest/stress or a stress/rest protocol. Both phases are necessary to accurately differentiate between ischemic and necrotic myocardium. Generally, static rest perfusion evaluation is derived from the anatomical acquisition of the coronary arteries; otherwise, a dynamic perfusion acquisition in both stress and rest states can be performed for quantitative coronary flow reserve measurements.<sup>28</sup>

The stress CTP scan is acquired during drug-induced arteriolar vasodilation (using dipyridamole, adenosine, or regadenoson) by both direct and endothelium-mediated mechanisms with a 3.5- to 4-fold increase in myocardial blood flow.<sup>10</sup> Adenosine nonselectively activates 4 receptor subtypes: A1, A2A, A2B, and A3, of which only A2A receptor activation vasodilates the coronary arterial beds, increases myocardial blood flow, and causes sympathoexcitation; the activation of the other receptors produces short-term undesirable side effects.<sup>29</sup> Dipyridamole increases endogenous adenosine levels by reducing its uptake from endothelial cells.<sup>10</sup> Both adenosine and dipyridamole may cause bronchospasm in patients with asthma and chronic obstructive pulmonary disease, while the newly introduced regadenoson, a selective A2A receptor agonist, may be safely used in these patients.<sup>29</sup> Other common

contraindications are severe AV block without PM, sinus bradycardia, systemic hypotension (blood pressure < 90 mmHg), and severe carotid stenosis. These drugs, by dilating the small resistance arterioles, reduce the perfusion pressure beyond the stenosis and, by increasing subepicardial blood flow, suppress the autoregulation mechanism (transmural coronary steal phenomenon). This results in a progressive reduction of the downstream flow as the entity of the stenosis increases.<sup>10,12</sup> All these agents have demonstrated good sensitivity and specificity; dipyridamole has the advantage of being inexpensive but has a longer vasodilation effect (several minutes instead of a few seconds with adenosine) that requires aminophylline antagonism (slow intravenous injection of 50 mg to 250 mg).<sup>12</sup> Complications are related to systemic vasodilation (tachycardia, hypotension, flushing, headache, and dizziness) and to the induction of myocardial ischemia (chest pain, dyspnea, ST-segment depression), ventricular tachycardia or transient atrio-ventricular block.<sup>12,29</sup> Before the examination, patients are advised to avoid drug antagonists such as methylxanthines contained in products such as coffee, tea, chocolate, energy drinks, or bronchodilators.<sup>9</sup> Dobutamine, a synthetic  $\beta_1$ - and  $\beta_2$ -receptor agonist, is commonly used in stress echocardiography for wall motion analysis and currently has no clinical role in CTP imaging.<sup>10,12</sup>

Two intravenous access sites are required to inject the stress agent and contrast media. Adenosine is infused at a standard rate of 0.14 mg/kg/min for 3 to 5 minutes with an infusion pump, while dipyridamole is infused in a dose of 0.56 mg/kg to 0.84 mg/kg over a 4 to 6 minute period.<sup>10,12</sup> Conversely, regadenoson can be administered in a single dose (400  $\mu$ g).<sup>29</sup> During the examination, heart rate is constantly monitored with a 12-lead ECG as well as blood pressure and oxygen saturation. The patient is repeatedly asked about the occurrence of any symptoms, which generally disappear when the drug injection is suspended or when an antagonist is administered.

Several protocols have been proposed and are published in the literature with their advantages and disadvantages (Figure 2).<sup>9,12</sup> The stress/rest CTP protocol, which allows more sensitive detection of ischemia, should preferably be used in patients with a high pretest probability of CAD or with known CAD, in whom extensive calcifications, multivessel disease or prior stent implantation may reduce coronary CTA accuracy in the evaluation of CAD. Conversely, the rest/stress CTP protocol should be the first choice in patients with a low-to-intermediate pretest probability of CAD, which allows discontinuation of the protocol when absent or minimal CAD is detected during the rest phase, reserving pharmacologic stress for patients with moderate-to-severe CAD (Figure 2).<sup>9,12</sup>

Although it is still experimental, a late sequence at 8 to 10 minutes can be added without further contrast material injection to reveal the presence of late myocardial enhancement, which indicates nonviable myocardium; low voltage (70–80–90–100 kV) protocols should be preferred due to the specific characteristic CT attenuation spectrum of iodine with high attenuation at low photon energies.<sup>23</sup> However, a late-enhancement scan is not mandatory in clinical practice due to the relatively poorer signal-to-noise and contrast-to-noise ratios of CT compared with MRI and the difficulty of assessing the transmural extent of the infarct.<sup>12,24</sup>

### DATA POSTPROCESSING

#### Qualitative and Static Quantitative Analysis

Stress CTP qualitative analysis is performed by visual analysis of the images acquired during stress and rest conditions, using a

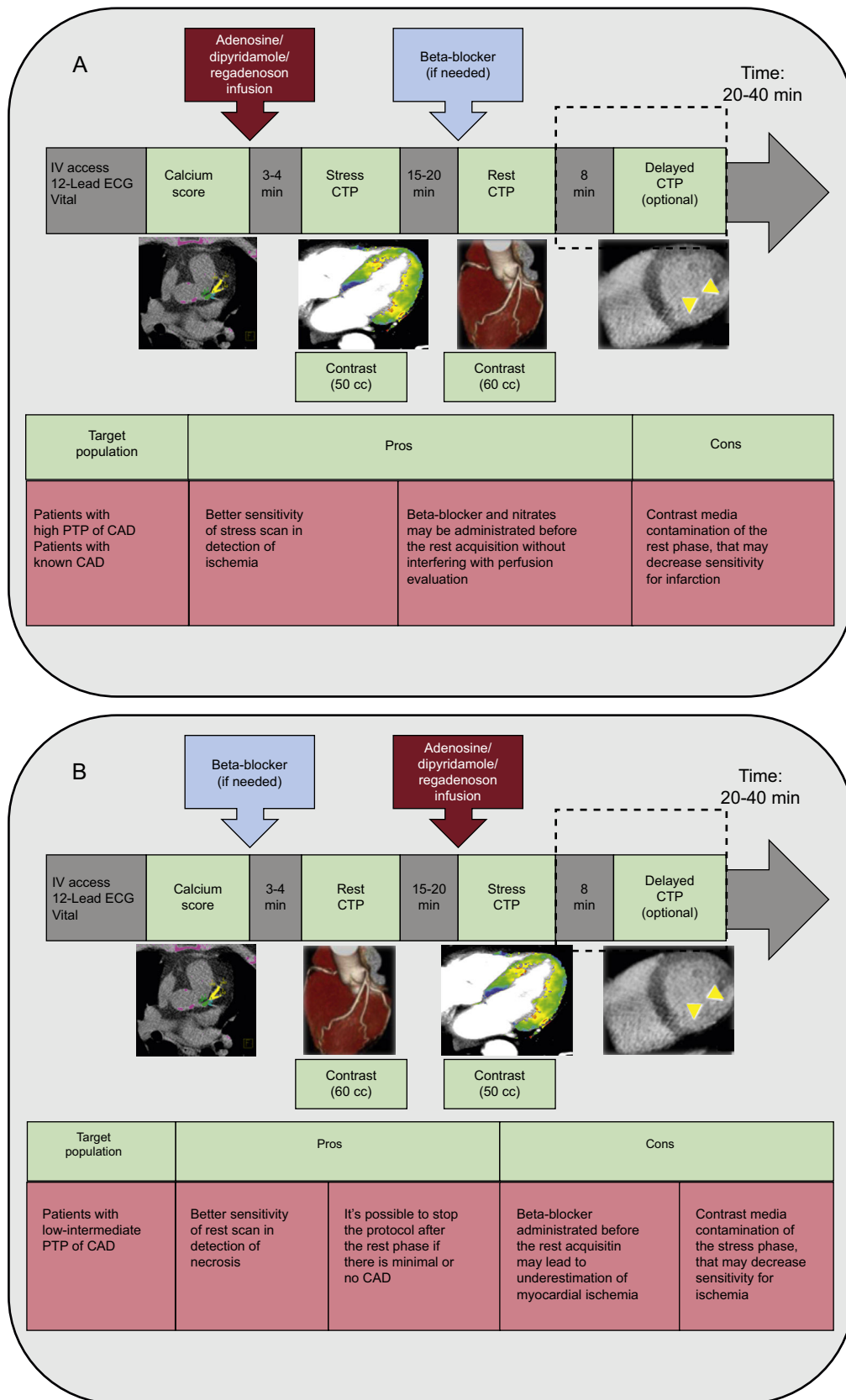


**Figure 2.** Stress-rest (A) and rest-stress (B) computed tomography myocardial perfusion protocols with advantages (pros) and disadvantages (cons). CTP, computed tomography perfusion imaging; CAD, coronary artery disease; ECG, electrocardiogram; IV, intravenous; PTP, pre-test probability of coronary artery disease.



standard of normality learned with experience. Images are interpreted based on the presence, location, and extension of the perfusion defect using standard cardiac long-axis and short-axis planes.<sup>30</sup> Thick multiplanar reconstruction of approximately 5 mm to 8 mm is usually preferred to optimize the contrast-to-noise ratio.<sup>12,30</sup> Qualitative assessment may be aided by evaluation of myocardial attenuation through measurements of the signal density levels within the myocardium. Automatic software employing “bull’s eye” plot of the transmural perfusion ratio (an endocardial-to-mean epicardial ratio of attenuation values), a semiquantitative index parameter initially validated for stress MRI, has been implemented to aid CTP analysis; however, it seems to be unreliable in the presence of prior infarction or significant beam-hardening or motion artifacts.<sup>30</sup>

In addition to qualitative analysis, the DE technique also allows quantitative analysis. From the raw data of the DE scan, 2 datasets at different kV are extracted, obtaining a merged dataset combining the reduced noise of the high energy level (140–150 kV) together with the high contrast resolution of the low energy level (80–90–100 kV), resulting in better differentiation of normal and hypoperfused myocardium.<sup>23</sup> By exploiting the DE information, a color-coded iodine distribution map—a surrogate marker of myocardial blood supply—may be obtained and overlapped with the virtual-noncontrast reconstruction (Figure 3).<sup>13,23</sup> The DE technique allows quantification of the per-voxel amount of iodine concentration within the myocardium expressed in mg/mL (Figure 3), a surrogate marker of myocardial blood supply.<sup>23</sup> Furthermore, due to its ability to generate monochromatic image reconstructions, the DE technique has been shown to mitigate or even eliminate beam

hardening artifacts related to cardiac geometry and iodinated contrast material occasionally resembling perfusion defects and commonly observed at the left ventricular posterobasal wall.<sup>9</sup>

### Dynamic Quantitative Analysis

Dynamic CTP imaging allows either a semiquantitative or a fully quantitative perfusion analysis.<sup>9</sup> Simple semiquantitative metrics, in a manner similar for stress MRI perfusion, allow for evaluation of blood flow kinetic parameters derived from the upslope of the TAC (time-to-peak, peak enhancement, upslope, and the area under the curve).<sup>9,10,26,28</sup> Since semiquantitative analysis needs computation of only the upslope part of the TAC, a lesser temporal sampling is required with a reduced radiation dose. Conversely, absolute myocardial perfusion quantification requires a complete first-pass coverage of the myocardium and is based on a dedicated algorithm that has been successfully used previously in MRI studies.<sup>9,10</sup> For a quantitative analysis using a DSCT scanner, a modified parametric deconvolution technique based on a 2-compartment model of intra- and extravascular space to fit the TAC is used.<sup>9,28</sup> The volumetric images dataset (≈10–15 sets of data) is processed using dedicated commercial perfusion software on a standard workstation (Syngo VPCT body-myocardium, Siemens Healthcare; Erlangen, Germany). After double-sampling of the AIF (arterial input function), the mathematical elaboration of the TAC enables calculation of the myocardial blood flow (MBF) in mL/100 mL/min and the myocardial blood volume (MBV) in mL/100 mL of each voxel, generating a 3D color-coded map

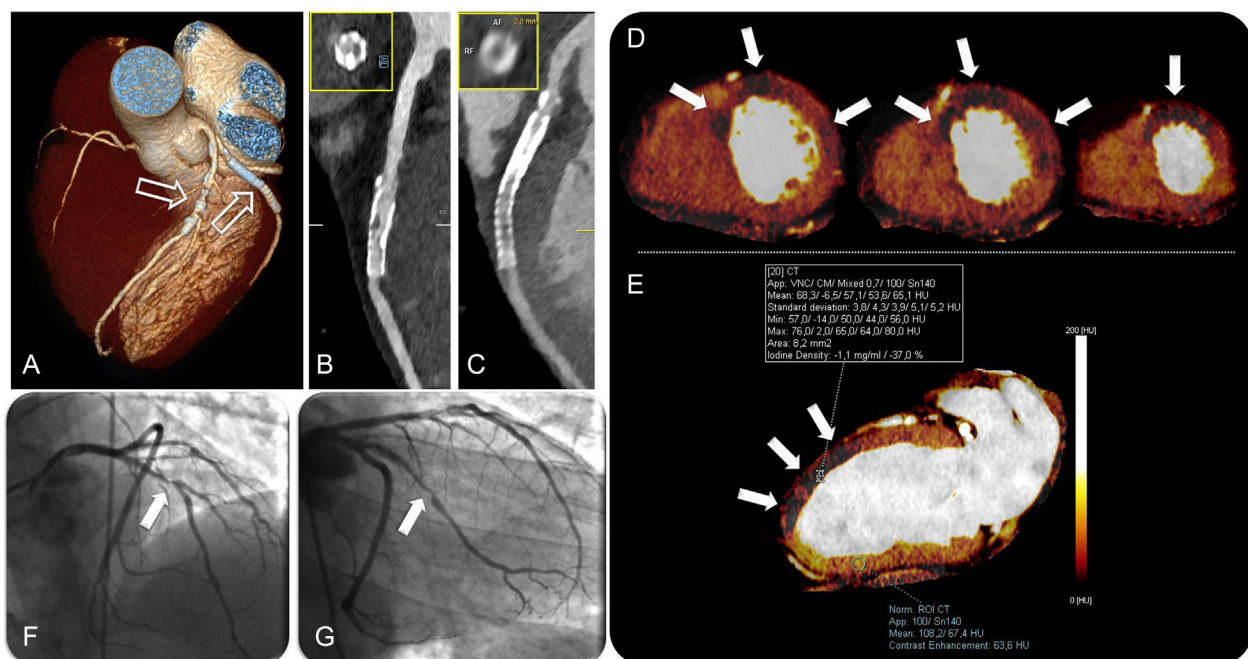


**Figure 3.** A three-dimensional volume rendered computed tomography image (A) showing a stent in the middle segment of the left anterior descending artery and double stenting in the proximal main obtuse marginal branch (arrows). Curved planar reformations of the left anterior descending artery (B) and the obtuse marginal branch (C) with the corresponding perpendicular views, showing in-stent restenosis. Myocardial short-axis color-coded iodine distribution maps of computed tomography dual-energy perfusion imaging from middle to apical segments show perfusion defects at the antero-septal, anterior, antero-lateral and lateral wall corresponding to the territory of the left anterior descending artery and left circumflex artery (arrows in D). Quantitative analysis of the dual-energy map at the level of the anterior wall (arrows) shows a 37% reduction in iodine content with respect to the remote myocardium at the inferior wall (E). Invasive coronary angiography confirmed the in-stent restenosis of the left anterior descending artery (arrow in F) and the obtuse marginal branch (arrow in G). AF, atrial fibrillation; CT, computed tomography; RF, radiofrequency; ROI, region of interest.

representation (Figure 4). Myocardial blood flow and MBV are computed according to the following equations:

$$\text{MBF} = \text{max slope (tissue TAC)} / \text{maximum (AIF)}$$

$$\text{MBV} = \text{maximum (tissue TAC)} / \text{maximum (AIF)}$$

Semiautomated software enabling a polar plot display of the modified 17-segment American Heart Association myocardial model is now available, with a substantially reduced analysis times and improvement in the standardization of the perfusion analysis.

## IMAGE INTERPRETATION

Similar to SPECT image and MRI interpretation, demonstration of a stress perfusion defect partially or totally reversible at rest indicates the presence of ischemic but viable myocardium; conversely, a matching defect on stress and rest images indicates a fixed defect consistent with the presence of myocardial necrosis (Figure 5).<sup>12,30</sup> The DE CTP technique, by means of 3-dimensional color-coded map representation of the static distribution of the contrast media during the time-frame of image acquisition,<sup>13,23</sup> shows a reduced iodine content in the ischemic or necrotic myocardium compared with the remote myocardium (Figure 3).

Dynamic stress CTP demonstrates reduced MBF and MBV in the segments corresponding to the perfusion defects, due to inducible ischemia or infarction (Figure 6). Furthermore, analysis of TAC allows differentiation of ischemic from necrotic myocardium. Ischemic but viable myocardium shows a decreased wash-in with a delayed and reduced peak enhancement and a conserved

wash-out compared with remote myocardium, whereas necrotic myocardium demonstrates a reduction in both wash-in and wash-out rates in the areas of scarring and necrosis (Figure 6). The integration of CTP analysis with coronary anatomical data is a crucial step for image interpretation and enables determination of whether a perfusion defect matches a region supplied by a stenotic coronary artery, thus determining the hemodynamic significance of coronary lesions (Figure 6). It is important to be aware of the variation of the vascular territory distribution in myocardial perfusion, which accounts for coronary anatomy variability. Moreover, reversible perfusion defects can be localized in the distribution territory of normal epicardial coronary arteries if there is microvascular and/or endothelial dysfunction.<sup>10,11</sup>

Iodinated contrast media, as well as Gd-based contrast agents used in MRI, are trapped and accumulate in the intracellular space of irreversibly damaged myocytes after myocardial infarction or in the expanded extracellular space due to fibrous scar tissue: these necrotic/fibrotic lesions can be demonstrated as hyperdense areas (hyper-enhancement) in a late sequence obtained 8 to 10 minutes after contrast media injection (Figure 7).<sup>24</sup>

## DOSE

During the last decade, several technological improvements have allowed a drastic reduction in the dose profile associated with coronary CTA together with an improvement in image quality. Accordingly, from an initial 20 mSv, the dose can now be reduced as low as 2 mSv or less by means of prospective ECG triggering, including the high-pitch spiral and iterative reconstruction methods.<sup>21,22</sup>

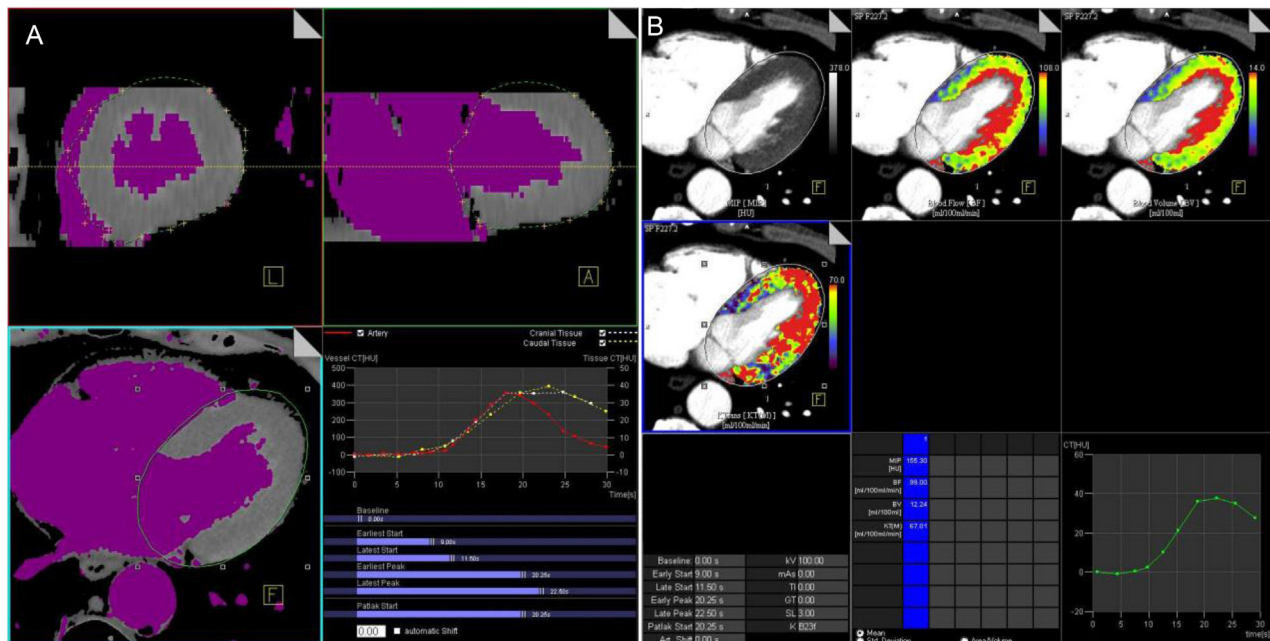


**Figure 4.** A: dynamic volumetric images datasets ( $\approx 10$ -15 sets of data) obtained with a second-generation dual-source 128 slice computed tomography scanner are processed with dedicated volume perfusion software. The algorithm double-sampled the arterial input function from regions of interest that were placed in the descending aorta at the cranial and caudal ends of the 2 image stacks, and combined into one arterial input function that has twice the sampling rate of the tissue time-attenuation curve. B: for each voxel, estimated myocardial blood flow (mL/100 mL/min) and myocardial blood volume (mL/100 mL) may be calculated by parametric deconvolution technique based on a 2-compartment model of intra- and extravascular space to fit the time attenuation curve. Other hemodynamic parameters can be derived, such as the transit-constant ( $K_{trans}$ , mL/100 mL/min), which describes permeability by calculating volume transfer between blood plasma and the extracellular extravascular space. Myocardial perfusion is represented with a 3-dimensional color-coded map.

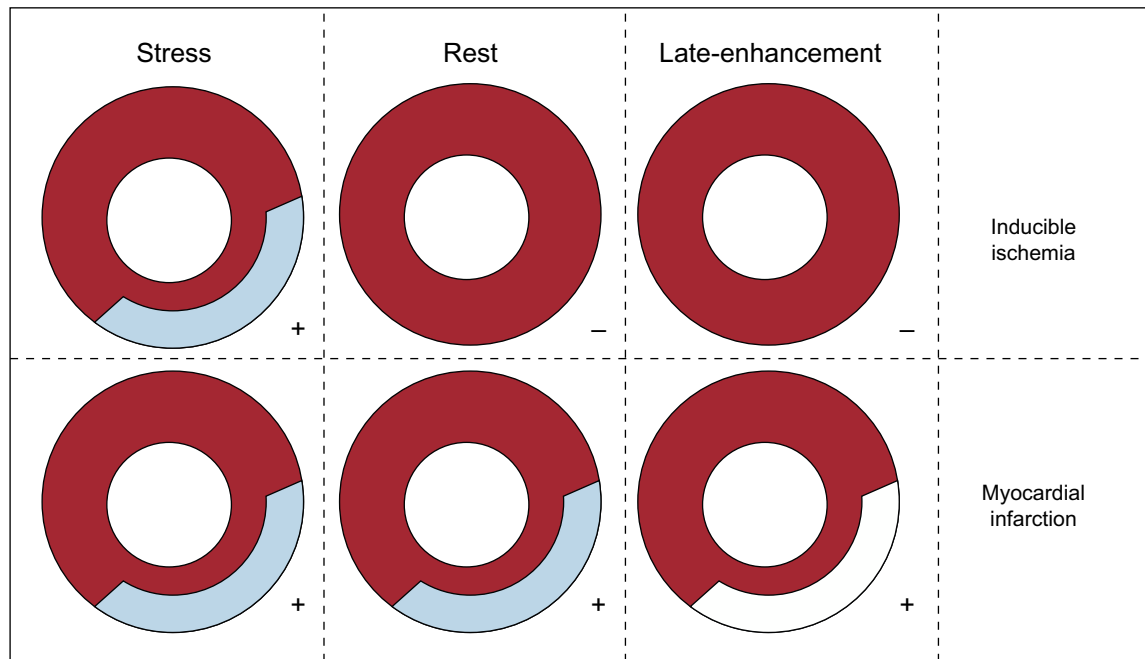


**Figure 5.** Guide to computed tomography myocardial perfusion imaging analysis. The demonstration of a stress perfusion defect partially or totally reversible at rest indicates the presence of ischemic but viable myocardium (inducible ischemia); when the perfusion defect persists at rest imaging it indicates the presence of myocardial infarction.

Tables 1 and 2 show the radiation dose, scanning protocols, and diagnostic accuracy of static CTP. The reported effective dose is in the range of 4.2 mSv to 7.7 mSv with the DE modality and is 5 mSv or less with the prospective ECG-gating monoenergetic technique, approaching 1 mSv with the high-pitch spiral acquisition of the DSCT scanner system (Tables 1 and 2). Accordingly, a complete

stress/rest protocol by means of high-pitch 128-slice DSCT scanner may result in a radiation dose as low as 2.5 mSv, while maintaining a sensitivity of 96% and a specificity of 88% compared with cardiac MRI on a vessel level.<sup>21</sup> Conversely, the effective dose of dynamic CTP is fairly variable, ranging from 3.8 mSv<sup>16</sup> to 12.5 mSv,<sup>27</sup> and is strictly dependent on

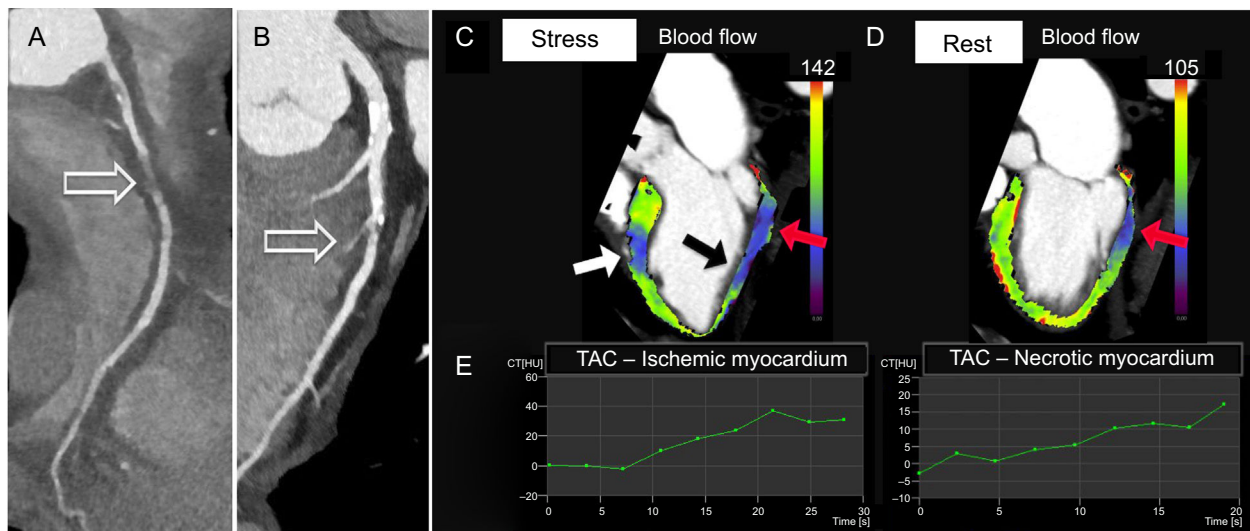


**Figure 6.** Curved planar reformation demonstrating chronic total occlusion of the proximal-mid right coronary artery (arrow in A) and a critical stenosis (> 70%) of the middle segment of the left anterior descending artery due to a mixed atherosclerotic plaque with involvement of the second septal perforating branch (arrow in B). Three-dimensional color-coded oblique 2-chamber computed tomography perfusion images at stress (C) and rest (D) show a reversible perfusion defect in the territory of the left anterior descending artery (middle antero-septal wall, color-coded in blue, white arrow in C), consistent with inducible ischemia, and a fixed perfusion defect in the territory of the right coronary artery (proximal inferior wall color-coded in blue-violet, red arrows in C and D), indicating myocardial necrosis. Note also a reversible defect in the territory of the right coronary artery (middle inferior wall, color-coded in blue, black arrow in C) indicating peri-infarct ischemia. The corresponding tissue time-attenuation curves of the ischemic (E, left image) and necrotic (E, right image) myocardium, respectively at the antero-septal and inferior wall, demonstrate a decreased wash-in with a delayed and reduced peak enhancement, especially in the area of scarring. During stress, a significant reduction was observed in both myocardial blood flow and myocardial blood volume of the necrotic (blood flow =  $50 \pm 14$  mL/100 mL/min; blood volume =  $7 \pm 2$  mL/100 mL) and ischemic (blood flow =  $65 \pm 15$  mL/100 mL/min; blood volume =  $10 \pm 2$  mL/100 mL) myocardium. TAC, time attenuation curve.



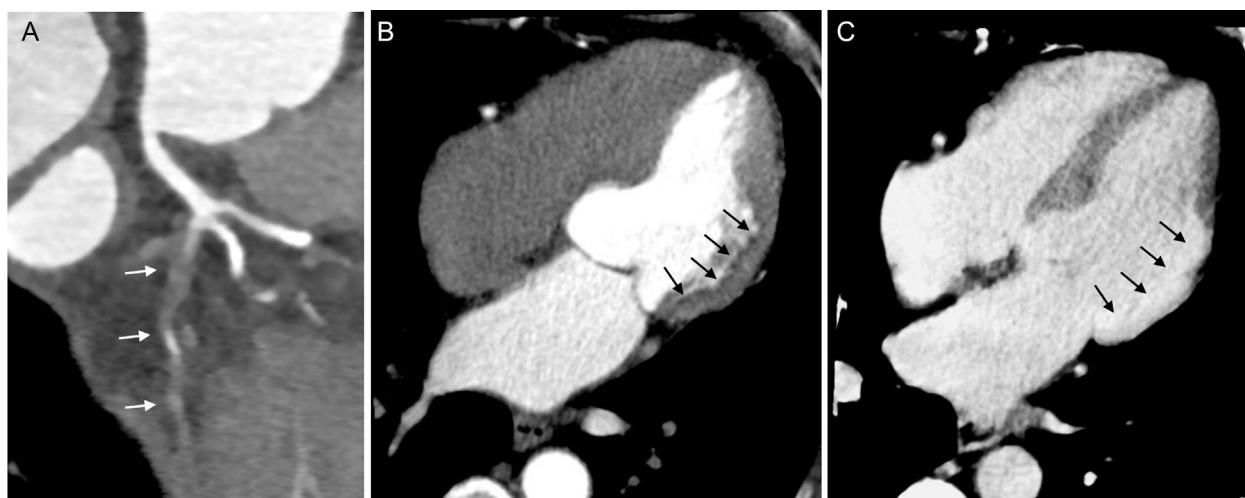


**Figure 7.** Curved planar reformation demonstrating chronic total occlusion at the ostium of the left circumflex artery (arrows, A). A 4-chamber rest computed tomography perfusion image acquired during first-pass enhancement showing a large perfusion defect at the lateral wall (arrows, B) in the territory of the left circumflex artery. Corresponding 4-chamber late-enhancement image obtained at 8 minutes using a low voltage (80 kV) protocol demonstrating hyper-enhancement due to myocardial necrosis (arrows, C).

protocol optimization<sup>16</sup> (Table 3). As a result, a combined rest/stress dynamic CTP study with 100 kV can require a mean radiation dose of 18 mSv.<sup>28</sup> This value may be consistently decreased using recent technical developments, including the low voltages (70 kV to 80 kV) acquisition and iterative reconstruction.<sup>49,50</sup>

Based on the above data, stress CTP can be considered competitive regarding the overall dose compared with SPECT imaging (dose of 10 mSv for <sup>99m</sup>Tc and 20 mSv to 40 mSv for scintigraphy with <sup>201</sup>Tl),<sup>22</sup> allowing the integration of functional and anatomical data in a single examination.

## ACCURACY

Multiple single-center studies and the first multicenter trials have shown that stress CTP provides good diagnostic accuracy for the detection of myocardial perfusion defects by both static monoenergetic and DE modalities (Tables 1 and 2). In particular, Ko et al<sup>13</sup> have demonstrated the higher accuracy of DE CTP study compared with coronary CTA examination alone in detecting significant stenosis according to conventional coronary angiography. In a recent study, by comparing the accuracy of different acquisition protocols with the DE technique and SPECT, Meinel et al<sup>24</sup> concluded that an examination including both stress and rest DE CTP is the modality of choice to reveal perfusion defects, with a sensitivity of 99%, specificity of 97%, positive predictive value of 92%, and negative predictive value of 100%; late-enhancement acquisition did not significantly improve diagnostic performance.<sup>24</sup> An ongoing prospective, multicenter study, the DECIDE-Gold trial, which evaluates the accuracy of rest-stress DE CTP imaging compared with invasive FFR (primary endpoints) and functional imaging (secondary endpoints), will improve the current evidence on DE CTP in the detection of myocardial ischemia.<sup>51</sup>

The CORE 320 study, a prospective multicenter international trial using the 320-detector scanner with 381 participants, has evaluated the diagnostic accuracy of combined coronary CTA and static adenosine-stress CTP compared with invasive angiography and SPECT. The study concluded that the overall performance of stress CTP imaging in the diagnosis of anatomic coronary stenosis

( $\geq 50\%$ ) was higher than that of SPECT and was driven in part by the higher sensitivity for left main and multivessel disease.<sup>36</sup> According to the CORE320 data, when combined with coronary CTA, myocardial CTP analysis substantially increased specificity and overall accuracy in identifying flow-limiting stenosis (CAD  $\geq 50\%$ ) as determined by invasive coronary angiography and SPECT.<sup>35,38</sup> These findings were consistent among patients with and without previous CAD, both in per-patient and in per-vessel analyses.<sup>35,38</sup> Another recent randomized, multicenter, multi-vendor CTP study with regadenoson in 110 participants, conducted at 11 sites in the United States using 6 different CT scanners, has demonstrated the noninferiority of the static CTP protocol in detecting perfusion defects with respect to SPECT as the reference standard, with high sensitivity and specificity of 90% and 82%, respectively.<sup>39</sup> Moreover, as in the CORE320 trial, regadenoson CTP provides improved diagnostic accuracy over CTA alone for the detection of myocardial ischemia.<sup>39</sup>

The software-derived transmural perfusion ratio and other index parameters such as the myocardial reserve index (difference in attenuation between the stress and rest phases) have been introduced as useful semiquantitative parameters for static myocardial CTP; however, they have shown lower diagnostic accuracy than standard visual qualitative analysis, especially when visual perfusion was added to the coronary CTA information.<sup>32,38</sup>

Regarding the diagnostic accuracy of dynamic stress CTP, data obtained from animal model-based studies have been very encouraging, demonstrating a good correlation with fluorescent microsphere measurements and histopathology (Table 4). Preliminary human studies confirmed the good diagnostic performance of dynamic CTP compared with well-established noninvasive functional methods such as SPECT and perfusion-MRI, and with the gold-standard, invasive FFR (Table 3). Indeed, CTP imaging added the possibility of improving the overall diagnostic accuracy of coronary CTA, particularly in the interpretation of intermediate stenosis.<sup>47,48</sup>

By means of dynamic CTP imaging, different absolute MBF cut-off values ranging from 75 mL/100 mL/min to 103.1 mL/100 mL/min with a DSCT scanner system and as high as 164 mL/100 mL/min using a 256-slices CT scanner have been proposed to distinguish between ischemic and nonischemic myocardium compared with invasive FFR.<sup>26,44,48,56,57</sup> The lack of



**Table 1**  
Static Computed Tomography Perfusion Imaging

Author	Year	No.	Scanner	Dose, mSv	Stressor, dose	Analysis	Reference	SE, %	SP, %	PPV, %	NPV, %
Blankstein et al <sup>17</sup>	2009	34	DS 1G	9.10	Adenosine (0.14 mg/kg/min)	Visual	SPECT (for vessel)	84	80	71	90
Rocha-Filo et al <sup>18</sup>	2010	35	DS 1G	9.80	Adenosine (0.14 mg/kg/min)	Visual	QCA (for vessel)	91	91	86	93
Feuchtnner et al <sup>21</sup>	2011	30	DS 2G	0.93	Adenosine (0.14 mg/kg/min)	Visual	MRI 1.5 T (for vessel)	96	88	93	94
Cury et al <sup>31</sup>	2011	26	64-detector CT	14.40 <sup>a</sup>	Dipyridamole (0.56 mg/Kg)	Visual	SPECT (for patient)	94	78	89	87
Ko et al <sup>32</sup>	2012	40	320-detector CT	4.50	Adenosine (0.14 mg/kg/min)	TPR	FFR (for vessel)	74	66	56	81
						Visual <sup>b</sup>	FFR (for vessel)	87	95	89	94
George et al <sup>19</sup>	2012	50	320-detector CT	7.00	Adenosine (0.14 mg/kg/min)	TPR	SPECT (for patient)	72	91	81	85
Nasis et al <sup>20</sup>	2013	20	320-detector CT	4.80	Adenosine (0.14 mg/kg/min)	Visual <sup>b</sup>	QCA + SPECT (for patient)	94	98	94	98
Bettencourt et al <sup>33</sup>	2013	101	64-detector CT	5.00 <sup>a</sup>	Adenosine (0.14 mg/kg/min)	Visual <sup>b</sup>	FFR (for patient)	89	83	80	90
							MRI 1.5 T (for patient)	67	95	91	78
Wong et al <sup>34</sup>	2014	75	320-detector CT	4.80	Adenosine (0.14 mg/kg/min)	Visual + TAG <sup>b</sup>	FFR (for vessel)	97	84	76	98
Rochitte et al (CORE320 study) <sup>35</sup>	2014	381	320-detector CT	5.31	Adenosine (0.14 mg/kg/min)	Semi-q	QCA + SPECT (for patient)	80	74	65	86
George et al (CORE320 study) <sup>36</sup>	2014	381	320-detector CT	NA	Adenosine (0.14 mg/kg/min)	Semi-q	QCA (for patient)	88	55	75	75
Yang et al <sup>37</sup>	2015	75	DS 2G	6.50	Adenosine (0.14 mg/kg/min)	Visual	FFR (for patient)	89	86	96	63
							FFR (for vessel)	80	95	92	87
Magalhaes et al (CORE320 study) <sup>38</sup>	2015	381	320-detector CT	NA	Adenosine (0.14 mg/kg/min)	Visual <sup>b</sup>	QCA + SPECT (for patient)	78	73	64	85
Cury et al (regadenoson crossover study) <sup>39</sup>	2015	110	Multivendor	17.70 <sup>a</sup>	Regadenoson (0.4 mg)	Semi-q	SPECT	90	82	53	97

1G, first generation; 2G, second generation; CT, computed tomography; DS, dual-source scanner; FFR, fractional flow reserve; MRI, magnetic resonance imaging; N°, patients' number; NA, nonassessable; NPV, negative predictive value; PPV, positive predictive value; QCA, quantitative coronary angiography; SE, sensitivity; Semi-q, semiquantitative analysis using a stress score; SP, specificity; SPECT, single-photon emission computed tomography; TAG, transluminal attenuation gradient; TPR, transmural perfusion ratio.

<sup>a</sup> Global radiation dose of the stress-rest protocol.

<sup>b</sup> Accuracy of computed tomography perfusion integrated with the coronary anatomic data.

**Table 2**  
Static Dual-energy Computed Tomography Perfusion Imaging

Author	Year	No.	Scanner	Dose, mSv	Stressor, dose	Analysis	Reference	SE, %	SP, %	PPV, %	NPV, %
Ko et al <sup>13</sup>	2012	45	DS 1G	5.7	Adenosine (0.14 mg/kg/min)	Iodine map (for vessel)	QCA	89	74	80	85
Delgado et al <sup>14</sup>	2013	56	DS 2G	5.2	Adenosine (0.14 mg/kg/min)	Iodine map (for segment)	MRI 1.5T	76	99	89	98
Meinel et al <sup>24</sup>	2014	55	DS 2G	7.1	Adenosine (0.14 mg/kg/min) regadenoson (0.4 mg)	Iodine map (for segment)	SPECT	99	97	92	100
Kido et al <sup>40</sup>	2014	21	DS 1G-2G	7.7	Adenosine (0.16 mg/kg/min)	Iodine map (for vessel)*	QCA	67	92	84	82
Kim et al <sup>41</sup>	2014	50	DS 2G	6.5	Adenosine (0.14 mg/kg/min)	Iodine map (for segment)	MRI 1.5T	77	94	53	98
Ko et al <sup>42</sup>	2014	40	DS 1G	4.6	Adenosine (0.14 mg/kg/min)	Iodine map (for vessel)*	QCA + MRI 3T	87	79	71	91
Ko et al <sup>43</sup>	2014	100	DS 1G	4.2	Adenosine (0.14 mg/kg/min)	Iodine map (for vessel)*	QCA + MRI 1.5T and 3T	88	79	73	91

1G, first generation; 2G, second generation; CT, computed tomography; DS, dual-source scanner; MRI, magnetic resonance imaging; N°, patients' number; NPV, negative predictive value; PPV, positive predictive value; QCA, quantitative coronary angiography; SE, sensitivity; SP, specificity; SPECT, single-photon emission computed tomography.

\* Accuracy of computed tomography perfusion integrated with the coronary anatomic data.

**Table 3**  
Dynamic Computed Tomography Perfusion Imaging in Human Studies

Author	Year	N <sup>a</sup>	Scanner	Dose, mSv	Stressor	Reference	Analysis	SE, %	SP, %	PPV, %	NPV, %
Bastarrika et al <sup>27</sup>	2010	10	DS 2G	12.50	Adenosine (0.14 mg/kg/min)	MRI (segment)	Visual, semiq, quantitative MBF	86	98	94	96
Ho et al <sup>28</sup>	2010	35	DS 2G	9.10	Dipyridamole (0.56 mg/Kg in 4')	SPECT (segment)	Quantitative MBF	83	78	79	82
Bamberg et al <sup>44</sup>	2011	33	DS 2G	10.00	Adenosine (0.14 mg/kg/min)	FFR (vessel)	Quantitative MBF <sup>*</sup>	93	87	75	97
Wang et al <sup>45</sup>	2012	30	DS 2G	9.50	Adenosine (0.14 mg/kg/min)	QCA + SPECT (vessel)	Visual, quantitative MBF and MBV	100	76	54	100
Greif et al <sup>46</sup>	2013	65	DS 2G	9.70	Adenosine (0.14 mg/kg/min)	FFR (vessel)	Quantitative MBF	95	74	49	98
Huber et al <sup>26</sup>	2013	32	256-detector CT	9.50	Adenosine (0.14 mg/kg/min)	FFR (vessel)	Quantitative MBF	76	100	100	91
Bamberg et al <sup>47</sup>	2014	31	DS 2G	11.08	Adenosine (0.14 mg/kg/min)	MRI 3T (vessel)	Quantitative MBF and MBV	100	75	92	100
Rossi et al <sup>48</sup>	2014	80	DS 2G	9.40	Adenosine (0.14 mg/kg/min)	FFR (vessel)	Quantitative MBF	88	90	77	95

2G, second-generation; CT, computed tomography; DS, dual-source scanner; FFR, fractional flow reserve; MRI, magnetic resonance imaging; MBF, myocardial blood flow; MBV, myocardial blood volume; N<sup>a</sup>, patients' number; NPV, negative predictive value; PPV, positive predictive value; QCA, quantitative coronary angiography; SE, sensitivity; Semiq, semiquantitative analysis; SP, specificity; SPECT, single-photon emission computed tomography.

<sup>\*</sup> Accuracy of computed tomography perfusion integrated with the coronary anatomic data.

uniformity may be attributed to variation in study protocols, the use of different scanners, and mathematical algorithms.<sup>26,48,56</sup> More recently, a study by Meinel et al<sup>58</sup> has also demonstrated the utility of dynamic CTP with DSCT scanner in the quantitative assessment of global left ventricular perfusion. Whole-heart perfusion was lower in patients with perfusion defects and decreased with an increasing extent of obstructive CAD, demonstrating the clinical feasibility of differentiating patients with normal perfusion from patients with 3-vessel obstructive CAD causing balanced ischemia.<sup>58</sup>

Furthermore, a recent study has shown that a relative MBF measurement (an absolute MBF-to-remote MBF ratio) may outperform absolute measures of MBF with a superior correlation with invasive FFR for detecting hemodynamically significant coronary lesions.<sup>56</sup> Some results were recently confirmed in a retrospective multicenter registry of 137 patients, in which the MBF ratio allowed a superior discrimination of obstructive CAD as detected by CTA compared with absolute MBF.<sup>57</sup>

Although a relative MBF may correct for intra-individual systemic variations in MBF, numerous other factors are known to modify the inter- and intra-individual MBF: age, sex, body mass index, hemodynamic (comprising differences in vasodilator

responsiveness), anatomic, metabolic, myogenic, endothelial, and neural mechanisms acting at different levels of the vascular tree, and methodological aspects (variations in contrast dose and injection technique as well as scanning protocols and different scanner types).<sup>11,48,56</sup> Further studies are needed to confirm the superiority of the normalized measurement of the MBF or other potential physiologic parameters with respect to absolute quantitative metrics.

While a human study has shown similar high diagnostic accuracy for ischemia prediction as detected by FFR of the single-shot CTP and the MBF parameter derived from dynamic CTP,<sup>26</sup> a large animal study has demonstrated a significantly better performance of quantitative MBF compared with the static single-phase myocardial attenuation value.<sup>54</sup> In particular, a notable difference in accuracy was demonstrated at lower degree of stenosis (50%), thus resulting in better discriminatory power for dynamic CTP with respect to static CTP in detecting ischemic myocardium.<sup>54</sup>

The results of initial meta-analyses have confirmed the high accuracy of CTP, although significant heterogeneity was a potential limitation of these analyses.<sup>59,60</sup> In particular, a meta-analysis by Takx et al<sup>59</sup> evaluating the accuracy of different myocardial

**Table 4**  
Dynamic Computed Tomography Perfusion Imaging in Animal Studies

Author	Year	No.	Scanner	Protocol	Dose, mSv	Stressor	Reference	Analysis
Bamberg et al <sup>52</sup>	2012	7 pigs	DS 2G	Stress: CTP dynamic	10.60	Adenosine (0.14 mg/kg/min)	Microsphere MBF	Quantitative MBF
Rossi et al <sup>53</sup>	2013	7 pigs	DS 2G	Stress: CTP dynamic	17.10	Adenosine (0.50 mg/kg/min)	CBF and FFR	Quantitative MBF
Schwarz et al <sup>54</sup>	2013	6 pigs	DS 2G	Stress: CTP dynamic + flash	11.30 + 0.88	Adenosine (0.14 mg/kg/min)	Microsphere MBF	Quantitative MBF + attenuation values (HU)
Bamberg et al <sup>55</sup>	2014	12 pigs	DS 2G	Stress: CTP dynamic	NA	Adenosine (0.14 mg/kg/min)	Histopathology Microsphere MBF	Quantitative MBF, MBV, K <sub>trans</sub>

2G, second-generation; CBF, coronary blood flow; CTP, computed tomography perfusion; DS, Dual-Source scanner; FFR, fractional flow reserve; HU, Hounsfield unit; K<sub>trans</sub>, permeability constant; MBF, myocardial blood flow; MBV, myocardial blood volume; NA, nonassessable.

perfusion techniques in comparison with FFR, indicated that CTP performed similarly to MRI and positron emission tomography and better than SPECT and echocardiography. Pooled results of another meta-analysis including 22 studies (1507 patients) comparing CTP to reference standards, including invasive coronary angiography, SPECT, and MRI, showed acceptable diagnostic performance for all myocardial perfusion CTP techniques (static and dynamic CTP) with sensitivity ranging from 75% to 89% and specificity from 78% to 95%.<sup>60</sup>

## STRENGTHS AND LIMITATIONS

Stress CTP still has a number of limitations, some of which will eventually be overcome as CT technology improves. Optimal scan acquisition parameters and reconstruction methods, post-processing, and standardized interpretation of stress CTP are still under investigation. Beam hardening and motion artifacts may hamper the diagnostic accuracy of stress CTP, but correction algorithms that may mitigate these effects are readily available. Furthermore, radiation exposure is also likely to decrease as CT technology advances, for example by employing iterative reconstruction methods for dynamic CTP imaging without affecting image quality.<sup>50</sup> Stress CTP studies have been performed with and without beta-blockade, which may have influenced myocardial perfusion assessment. Finally, most of the current evidence on CTP comes from single-center studies with a limited number of enrolled patients. However, CTP has superior spatial resolution to SPECT, the most widely used functional imaging technique in routine clinical practice, which may allow detection of smaller, especially subendocardial perfusion defects. Furthermore, CTP provides “one-stop shop” imaging with the unique advantage of achieving integrated anatomic and functional evaluation in a single examination. These strengths potentially make CTP a more effective gatekeeper to invasive coronary angiography with better stratification of patients who would benefit from revascularization.

## CONCLUSIONS AND FUTURE PROSPECTS

The rapid technological progress in cardiac imaging has dramatically widened the application of CTA in the assessment of ischemic cardiomyopathy, enabling pharmacological stress myocardial CTP imaging. This modality is highly appealing and is able to improve diagnostic accuracy, particularly the specificity and positive predictive value of coronary CTA.

Stress CTP has the potential to evaluate a broad spectrum of coronary vascular dysfunction: from microvascular dysfunction related to cardiovascular risk factors and advanced diffuse nonobstructive atherosclerosis, to intermediate-to-severe stenosis or multivessel CAD. Stress CTP may increase diagnostic accuracy in the assessment of stent patency and diffusely calcified coronary tree.<sup>61,62</sup>

Further studies seem to be warranted to demonstrate the noninferiority of the static single-phase protocol with respect to dynamic stress CTP, since the dynamic time-resolved technique provides fully quantitative data but at the price of a higher dose due to the extended imaging time. It's probable that in the near future the choice of the optimal acquisition protocol and pattern for analysis to accurately assess the left ventricular myocardial perfusion will be driven by various factors, including technical aspects (type of imaging platform used) and patient-based variables (patient's physical condition, coronary status, and pretest probability of CAD).

Future prospects may include further technological improvements in both hardware (better sensitivity and a wider range of

the detector system, higher temporal and spatial resolution, and DE implementation) and software updates (enabling post-processing standardization which is needed for more accurate and reproducible data analysis and successful clinical implementation).

We are positive about the future usefulness of myocardial CTP. Even though the diagnostic validation of CTP is still ongoing, the potential role of CTP as a diagnostic tool in detecting hemodynamically significant CAD is promising and merits further investigation. Results from the first controlled studies are outstanding and encouraging, but, as technology continues to evolve, further larger, multicenter trials are warranted to demonstrate the effective clinical role of CTP and its economic impact in relation to other functional imaging modalities.

Finally, although myocardial perfusion is historically a strong estimator of outcome, the prognostic implication of perfusion defects as assessed by CTP must be completely defined. We thus eagerly await studies assessing the prognostic value of CTP imaging for the prediction of future cardiac events, which will strengthen its diagnostic role in clinical practice.

## CONFLICTS OF INTEREST

None declared.

## REFERENCES

1. Yang L, Zhou T, Zhang R, Xu L, Peng Z, Ding J, et al. Meta-analysis: diagnostic accuracy of coronary CT angiography with prospective ECG gating based on step-and-shoot, Flash and volume modes for detection of coronary artery disease. *Eur Radiol*. 2014;24:2345–52.
2. Mahía-Casado P, García-Orta R, Gómez de Diego JJ, Barba-Cosials J, Rodríguez-Palomares JF, Aguadé-Bruix S. Novedades en imagen cardiaca 2014. *Rev Esp Cardiol*. 2015;68:129–35.
3. Descalzo M, Leta R, Rosselló X, Alomar X, Carreras F, Pons-Lladó G. Enfermedad coronaria subclínica por tomografía computarizada multidetector en población asintomática estratificada por nivel de riesgo coronario. *Rev Esp Cardiol*. 2013;66:504–5.
4. Raff GL, Chinnaiyan KM. Papel del angio-TAC coronario en la clasificación precoz de los pacientes con dolor torácico agudo. *Rev Esp Cardiol*. 2009;62:961–5.
5. Tonino PA, Fearon WF, De Bruyne B, Oldroyd KG, Leesar MA, Ver Lee PN, et al. Angiographic versus functional severity of coronary artery stenoses in the FAME study: fractional flow reserve versus angiography in multivessel evaluation. *J Am Coll Cardiol*. 2010;55:2816–21.
6. Boden WE, O'Rourke RA, Teo KK, Hartigan PM, Maron DJ, Kostuk WJ, et al.; COURAGE Trial Research Group. Optimal medical therapy with or without PCI for stable coronary disease. *N Engl J Med*. 2007;356:1503–16.
7. Frye RL, August P, Brooks MM, Hardison RM, Kelsey SF, MacGregor JM, et al.; BARI 2D Study Group. A randomized trial of therapies for type 2 diabetes and coronary artery disease. *N Engl J Med*. 2009;360:2503–15.
8. Van Werkhoven JM, Schuijff JD, Gaemperli O, Jukema JW, Boersma E, Wijns W, et al. Prognostic value of multislice computed tomography and gated single-photon emission computed tomography in patients with suspected coronary artery disease. *J Am Coll Cardiol*. 2009;53:623–32.
9. Rossi A, Merkus D, Klotz E, Mollet N, De Feyter PJ, Krestin GP. Stress myocardial perfusion: imaging with multidetector CT. *Radiology*. 2014;270:25–46.
10. Salerno M, Beller GA. Noninvasive assessment of myocardial perfusion. *Circ Cardiovasc Imaging*. 2009;2:412–24.
11. Duncker DJ, Koller A, Merkus D, Cauty Jr JM. Regulation of coronary blood flow in health and ischemic heart disease. *Prog Cardiovasc Dis*. 2015;57:409–22.
12. Techathit T, Cury RC. Stress myocardial CT perfusion: an update and future perspective. *JACC Cardiovasc Imaging*. 2011;4:905–16.
13. Ko SM, Choi JW, Hwang HK, Song MG, Shin JK, Chee HK. Diagnostic performance of combined noninvasive anatomic and functional assessment with dual-source CT and adenosine-induced stress dual-energy CT for detection of significant coronary stenosis. *AJR Am J Roentgenol*. 2012;198:512–20.
14. Delgado C, Vázquez M, Oca R, Vilar M, Trinidad C, Sanmartín M. Evaluación de la isquemia miocárdica con tomografía computarizada de doble fuente: comparación con la resonancia magnética. *Rev Esp Cardiol*. 2013;66:864–70.
15. Bischoff B, Bamberg F, Marcus R, Schwarz F, Becker HC, Becker A, et al. Optimal timing for first-pass stress CT myocardial perfusion imaging. *Int J Cardiovasc Imaging*. 2013;29:435–42.
16. Kim SM, Kim YN, Choe YH. Adenosine-stress dynamic myocardial perfusion imaging using 128-slice dual-source CT: optimization of the CT protocol to reduce the radiation dose. *Int J Cardiovasc Imaging*. 2013;29:875–84.

17. Blankstein R, Shturman LD, Rogers IS, Rocha-Filho JA, Okada DR, Sarwar A, et al. Adenosine-induced stress myocardial perfusion imaging using dual-source cardiac computed tomography. *J Am Coll Cardiol*. 2009;54:1072–84.
18. Rocha-Filho JA, Blankstein R, Shturman LD, Bezerra HG, Okada DR, Rogers IS, et al. Incremental value of adenosine-induced stress myocardial perfusion imaging with dual-source CT at cardiac CT angiography. *Radiology*. 2010;254:410–9.
19. George RT, Arbab-Zadeh A, Miller JM, Vavere AL, Bengel FM, Lardo AC, et al. Computed tomography myocardial perfusion imaging with 320-row detector computed tomography accurately detects myocardial ischemia in patients with obstructive coronary artery disease. *Circ Cardiovasc Imaging*. 2012;5:333–40.
20. Nasis A, Ko BS, Leung MC, Antonis PR, Nandurkar D, Wong DT, et al. Diagnostic accuracy of combined coronary angiography and adenosine stress myocardial perfusion imaging using 320-detector computed tomography: pilot study. *Eur Radiol*. 2013;23:1812–21.
21. Feuchtner G, Goetti R, Plass A, Wieser M, Scheffel H, Wyss C, et al. Adenosine stress high-pitch 128-slice dual-source myocardial computed tomography perfusion for imaging of reversible myocardial ischemia: comparison with magnetic resonance imaging. *Circ Cardiovasc Imaging*. 2011;4:540–9.
22. Maffei E, Martini C, De Crescenzo S, Arcadi T, Clemente A, Capuano E, et al. Low dose CT of the heart: a quantum leap into a new era of cardiovascular imaging. *Radiol Med*. 2010;115:1179–207.
23. Vlieghehart R, Pelgrim GJ, Ebersberger U, Rowe GW, Oudkerk M, Schoepf UJ. Dual-energy CT of the heart. *AJR Am J Roentgenol*. 2012;199(5 Suppl):S54–63.
24. Meinel FG, De Cecco CN, Schoepf UJ, Nance Jr JW, Silverman JR, Flowers BA, et al. First-arterial-pass dual-energy CT for assessment of myocardial blood supply: do we need rest, stress, and delayed acquisition? Comparison with SPECT. *Radiology*. 2014;270:708–16.
25. Morsbach F, Gordic S, Desbiolles L, Husarik D, Frauenfelder T, Schmidt B, et al. Performance of turbo high-pitch dual-source CT for coronary CT angiography: first ex vivo and patient experience. *Eur Radiol*. 2014;24:1889–95.
26. Huber AM, Leber V, Gramer BM, Muenzel D, Leber A, Rieber J, et al. Myocardium: dynamic versus single-shot CT perfusion imaging. *Radiology*. 2013;269:378–86.
27. Bastarrika G, Ramos-Duran L, Rosenblum MA, Kang DK, Rowe GW, Schoepf UJ, et al. Adenosine-stress dynamic myocardial CT perfusion imaging: initial clinical experience. *Invest Radiol*. 2010;45:306–13.
28. Ho KT, Chua KC, Klotz E, Panknin C. Stress and rest dynamic myocardial perfusion imaging by evaluation of complete time-attenuation curves with dual-source CT. *JACC Cardiovasc Imaging*. 2010;3:811–20.
29. Al Jaroudi W, Iskandrian AE. Regadenoson: a new myocardial stress agent. *J Am Coll Cardiol*. 2009;54:1123–30. Erratum in: *J Am Coll Cardiol*. 2009;54:1635.
30. Mehra VC, Valdiviezo C, Arbab-Zadeh A, Ko BS, Seneviratne SK, Cerri R, et al. A stepwise approach to the visual interpretation of CT-based myocardial perfusion. *J Cardiovasc Comput Tomogr*. 2011;5:357–69.
31. Cury RC, Magalhães TA, Paladino AT, Shiozaki AA, Perini M, Senra T, et al. Dipyridamole stress and rest transmural myocardial perfusion ratio evaluation by 64 detector-row computed tomography. *J Cardiovasc Comput Tomogr*. 2011;5:443–8.
32. Ko BS, Cameron JD, Leung M, Meredith IT, Leong DP, Antonis PR, et al. Combined CT coronary angiography and stress myocardial perfusion imaging for hemodynamically significant stenoses in patients with suspected coronary artery disease: a comparison with fractional flow reserve. *JACC Cardiovasc Imaging*. 2012;5:1097–111.
33. Bettencourt N, Ferreira ND, Leite D, Carvalho M, Ferreira Wda S, Schuster A, et al. CAD detection in patients with intermediate-high pre-test probability: low-dose CT delayed enhancement detects ischemic myocardial scar with moderate accuracy but does not improve performance of a stress-rest CT perfusion protocol. *JACC Cardiovasc Imaging*. 2013;6:1062–71.
34. Wong DT, Ko BS, Cameron JD, Leong DP, Leung MC, Malaipayan Y, et al. Comparison of diagnostic accuracy of combined assessment using adenosine stress computed tomography perfusion + computed tomography angiography with transluminal attenuation gradient + computed tomography angiography against invasive fractional flow reserve. *J Am Coll Cardiol*. 2014;63:1904–12.
35. Rochitte CE, George RT, Chen MY, Arbab-Zadeh A, Dewey M, Miller JM, et al. Computed tomography angiography and perfusion to assess coronary artery stenosis causing perfusion defects by single photon emission computed tomography: the CORE320 study. *Eur Heart J*. 2014;35:1120–30.
36. George RT, Mehra VC, Chen MY, Kitagawa K, Arbab-Zadeh A, Miller JM, et al. Myocardial CT perfusion imaging and SPECT for the diagnosis of coronary artery disease: a head-to-head comparison from the CORE320 multicenter diagnostic performance study. *Radiology*. 2014;272:407–16. Erratum in: *Radiology*. 2015;274:626.
37. Yang DH, Kim YH, Roh JH, Kang JW, Han D, Jung J, et al. Stress myocardial perfusion CT in patients suspected of having coronary artery disease: visual and quantitative analysis-validation by using fractional flow reserve. *Radiology*. 2015;276:715–23.
38. Magalhães TA, Kishi S, George RT, Arbab-Zadeh A, Vavere AL, Cox C, et al. Combined coronary angiography and myocardial perfusion by computed tomography in the identification of flow-limiting stenosis—The CORE320 study: An integrated analysis of CT coronary angiography and myocardial perfusion. *J Cardiovasc Comput Tomogr*. 2015;9:438–45.
39. Cury RC, Kitt TM, Feaheny K, Blankstein R, Ghoshhajra BB, Budoff MJ, et al. A randomized, multicenter, multivendor study of myocardial perfusion imaging with regadenoson CT perfusion vs single photon emission CT. *J Cardiovasc Comput Tomogr*. 2015;9:103–12. e1–2.
40. Kido T, Watanabe K, Saeki H, Shigemitsu S, Matsuda T, Yamamoto M, et al. Adenosine triphosphate stress dual-source computed tomography to identify myocardial ischemia: comparison with invasive coronary angiography. *Springerplus*. 2014;3:75.
41. Kim SM, Chang SA, Shin W, Choe YH. Dual-energy CT perfusion during pharmacologic stress for the assessment of myocardial perfusion defects using a second-generation dual-source CT: a comparison with cardiac magnetic resonance imaging. *J Comput Assist Tomogr*. 2014;38:44–52.
42. Ko SM, Park JH, Hwang HK, Song MG. Direct comparison of stress- and rest-dual-energy computed tomography for detection of myocardial perfusion defect. *Int J Cardiovasc Imaging*. 2014;30 Suppl 1:41–53.
43. Ko SM, Song MG, Chee HK, Hwang HK, Feuchtner GM, Min JK. Diagnostic performance of dual-energy CT stress myocardial perfusion imaging: direct comparison with cardiovascular MRI. *AJR Am J Roentgenol*. 2014;203:W605–13.
44. Bamberg F, Becker A, Schwarz F, Marcus RP, Greif M, von Ziegler F, et al. Detection of hemodynamically significant coronary artery stenosis: incremental diagnostic value of dynamic CT-based myocardial perfusion imaging. *Radiology*. 2011;260:689–98.
45. Wang Y, Qin L, Shi X, Zeng Y, Jing H, Schoepf UJ, et al. Adenosine-stress dynamic myocardial perfusion imaging with second-generation dual-source CT: comparison with conventional catheter coronary angiography and SPECT nuclear myocardial perfusion imaging. *AJR Am J Roentgenol*. 2012;198:521–9.
46. Greif M, Von Ziegler F, Bamberg F, Tittus J, Schwarz F, D'Anastasi M, et al. CT stress perfusion imaging for detection of haemodynamically relevant coronary stenosis as defined by FFR. *Heart*. 2013;99:1004–11.
47. Bamberg F, Marcus RP, Becker A, Hildebrandt K, Bauner K, Schwarz F, et al. Dynamic myocardial CT perfusion imaging for evaluation of myocardial ischemia as determined by MR imaging. *JACC Cardiovasc Imaging*. 2014;7:267–77.
48. Rossi A, Dharmapal A, Wragg A, Davies LC, Van Geuns RJ, Anagnostopoulos C, et al. Diagnostic performance of hyperaemic myocardial blood flow index obtained by dynamic computed tomography: does it predict functionally significant coronary lesions? *Eur Heart J Cardiovasc Imaging*. 2014;15:85–94.
49. Fujita M, Kitagawa K, Ito T, Shiraishi Y, Kurobe Y, Nagata M, et al. Dose reduction in dynamic CT stress myocardial perfusion imaging: comparison of 80-kV/370-mAs and 100-kV/300-mAs protocols. *Eur Radiol*. 2014;24:748–55.
50. Tao Y, Chen G-H, Hacker TA, Raval AN, Van Lysel MS, Speidel MA. Low dose dynamic CT myocardial perfusion imaging using a statistical iterative reconstruction method. *Medical Physics*. 2014;41:071914.
51. Truong QA, Knaapen P, Pontone G, Andreini D, Leipsic J, Carrascosa P, et al. Rationale and design of the dual-energy computed tomography for ischemia determination compared to “gold standard” non-invasive and invasive techniques (DECIDE-Gold): A multicenter international efficacy diagnostic study of rest-stress dual-energy computed tomography angiography with perfusion. *J Nucl Cardiol*. 2015;22:1031–40.
52. Bamberg F, Hinkel R, Schwarz F, Sandner TA, Baloch E, Marcus R, et al. Accuracy of dynamic computed tomography adenosine stress myocardial perfusion imaging in estimating myocardial blood flow at various degrees of coronary artery stenosis using a porcine animal model. *Invest Radiol*. 2012;47:71–7.
53. Rossi A, Uitterdijk A, Dijkshoorn M, Klotz E, Dharmapal A, Van Straten M, et al. Quantification of myocardial blood flow by adenosine-stress CT perfusion imaging in pigs during various degrees of stenosis correlates well with coronary artery blood flow and fractional flow reserve. *Eur Heart J Cardiovasc Imaging*. 2013;14:331–8.
54. Schwarz F, Hinkel R, Baloch E, Marcus RP, Hildebrandt K, Sandner TA, et al. Myocardial CT perfusion imaging in a large animal model: comparison of dynamic versus single-phase acquisitions. *JACC Cardiovasc Imaging*. 2013;6:1229–38.
55. Bamberg F, Hinkel R, Marcus RP, Baloch E, Hildebrandt K, Schwarz F, et al. Feasibility of dynamic CT-based adenosine stress myocardial perfusion imaging to detect and differentiate ischemic and infarcted myocardium in a large experimental porcine animal model. *Int J Cardiovasc Imaging*. 2014;30:803–12.
56. Kono AK, Coenen A, Lubbers M, Kurata A, Rossi A, Dharmapal A, et al. Relative myocardial blood flow by dynamic computed tomographic perfusion imaging predicts hemodynamic significance of coronary stenosis better than absolute blood flow. *Invest Radiol*. 2014;49:801–7.
57. Wichmann JL, Meinel FG, Schoepf UJ, Lo GG, Choe YH, Wang Y, et al. Absolute versus relative myocardial blood flow by dynamic CT myocardial perfusion imaging in patients with anatomic coronary artery disease. *AJR Am J Roentgenol*. 2015;205:W67–72.
58. Meinel FG, Ebersberger U, Schoepf UJ, Lo GG, Choe YH, Wang Y, et al. Global quantification of left ventricular myocardial perfusion at dynamic CT: feasibility in a multicenter patient population. *AJR Am J Roentgenol*. 2014;203:W174–80.



59. Takx RA, Blomberg BA, El Aidi H, Habets J, De Jong PA, Nagel E, et al. Diagnostic accuracy of stress myocardial perfusion imaging compared to invasive coronary angiography with fractional flow reserve meta-analysis. *Circ Cardiovasc Imaging*. 2015;8. Available at: <http://dx.doi.org/10.1161/CIRCIMAGING.114.002666>
60. Pelgrim GJ, Dorrius M, Xie X, Den Dekker MA, Schoepf UJ, Henzler T, et al. The dream of a one-stop-shop: Meta-analysis on myocardial perfusion CT. *Eur J Radiol*. 2015;84:2411–20.
61. Rief M, Zimmermann E, Stenzel F, Martus P, Stangl K, Greupner J, et al. Computed tomography angiography and myocardial computed tomography perfusion in patients with coronary stents: prospective intraindividual comparison with conventional coronary angiography. *J Am Coll Cardiol*. 2013;62:1476–85.
62. Sharma RK, Arbab-Zadeh A, Kishi S, Chen MY, Magalhães TA, George RT, et al. Incremental diagnostic accuracy of computed tomography myocardial perfusion imaging over coronary angiography stratified by pre-test probability of coronary artery disease and severity of coronary artery calcification: The CORE320 study. *Int J Cardiol*. 2015;201:570–7.